ACS Macro Letters

Letter

pubs.acs.org/macroletters

# Role of Localized Network Damage in Block Copolymer Toughened Epoxies

Carmelo Declet-Perez, Erica M. Redline,† Lorraine F. Francis, and Frank S. Bates*

Department of Chemical Engineering and Materials Science, University of Minnesota, Minneapolis, Minnesota 55455, United States

**ABSTRACT:** The underlying mechanisms responsible for the toughening of block copolymer modified thermoset epoxies are not completely understood. A current theory targets cavitation of the rubbery cores in dispersed micelles as the key event that triggers shear yielding, resulting in enhanced toughness. To evaluate this hypothesis, we prepared spherical micelle forming block copolymers with rubbery cores (prone to cavitation) and glassy cores (unable to cavitate). Surprisingly, both systems enhance fracture toughness, although the rubbery core micelles outperform the glassy core counterparts. This finding challenges previous deductions regarding the toughening mechanism. We propose that the mechanical integrity of the region immediately surrounding the micelle core is compromised by the presence of the corona blocks, facilitating local deformation of the matrix. We speculate that the compliant nature of the rubber amplifies this effect.

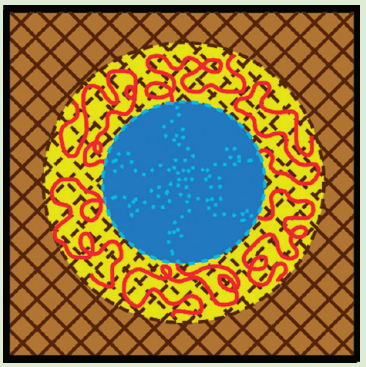

Improving the fracture resistance of epoxy resins without sacrificing desirable properties such as modulus and glass transition temperature has been a major challenge over the last 40 years. One of the latest toughening strategies involves the use of block copolymers as epoxy modifiers. When properly designed, block copolymers can self-assemble into a variety of structures in the uncured epoxy.[1−13] Disordered, micellar structures are formed when the block copolymer is present in low concentrations in the mixture.[2,7] Furthermore, these structures survive cure of the epoxy into a dense network, providing a robust approach for controlling the size, shape, and dispersion of the particles in the cross-linked matrix. While the effectiveness of this toughening approach has been well documented,[8,13−23] complete understanding of the underlying toughening mechanisms is still lacking. The purpose of this communication is to present new experimental evidence that challenges the current rationalization of toughening in block copolymer modified epoxies. This work highlights the role of the epoxy/block copolymer interface, or mixing region, and its contribution to the toughening mechanism. We suggest that the block copolymer effectively disrupts the local properties of the epoxy network allowing energy absorbing processes such as shear yielding to take place.

Recently, Liu et al. proposed that epoxies modified with spherical micelle forming diblock copolymers with a rubbery poly(ethylene-*alt*-propylene) core and poly(ethylene oxide) corona toughen through the same mechanism as traditional rubber modifiers.[17] This mechanism invokes matrix shear yielding as the primary energy absorbing process, triggered by cavitation of the nanoscale rubber domains. The sequence of events in the proposed toughening mechanism is based on the hypothesis that rubber cavitation relieves the triaxial constraint of the network allowing plastic deformation to occur (i.e., shear yielding occurs after the local stress state of the matrix changes from plane strain to plane stress). To evaluate this hypothesis we prepared a spherical micelle forming block copolymer with a rigid core to inhibit cavitation.

The structure of the epoxy systems and block copolymers used in this study are presented in Chart 1. Two epoxy systems were evaluated in this work, providing access to networks with varying properties (e.g., cross-link density and backbone flexibility). The main difference between these systems is the type of reactive groups in the hardener; phenols for CET and primary amines for Epon-JA. Poly(ethylene oxide) (PEO) was used as the "epoxy-miscible" block for both types of block copolymer, while the "epoxy-immiscible" block was varied to obtain different core properties. Poly(ethylene-*alt*-propylene) (PEP) produces a rubbery, compliant core, while polystyrene (PS) results in a glassy, rigid core.

Representative TEM images of block copolymer modified epoxies after full cure are presented in Figure 1. The block copolymers self-assemble into well dispersed spherical micelles as clearly observed in the micrographs. In both images PS-PEO was used as the modifier, producing narrowly distributed spheres with diameters of 20 nm.[24]

Figure 2a summarizes the $G_{1c}$ values obtained for the CET epoxy system, including previously reported results for PEP-PEO[21] and new data for PS-PEO. The molecular weight between cross-links ($M_c$) of the network was varied by changing the ratio of bisphenol A to THPE (Chart 1) in the formulation. A constant block copolymer loading of 5 wt % was used for all formulations. Clearly, the magnitude of improvement in $G_{1c}$ depends on the cross-link density for both the rubbery[21] and glassy core micelles. Although PS-PEO is less effective than PEP-PEO, the rigid, glassy core additive still imparts considerable toughness improvement, especially at higher $M_c$.

A related effect is shown for the Epon-JA system in Figure 2b, in this case with varying block copolymer concentration. Epon-JA

**Received:** December 10, 2011
**Accepted:** February 2, 2012
**Published:** February 9, 2012

   dx.doi.org/10.1021/mz200219y | *ACS Macro Lett.* 2012, 1, 338−342

**Chart 1. Structure of Epoxy Precursors and Block Copolymer Modifiers**

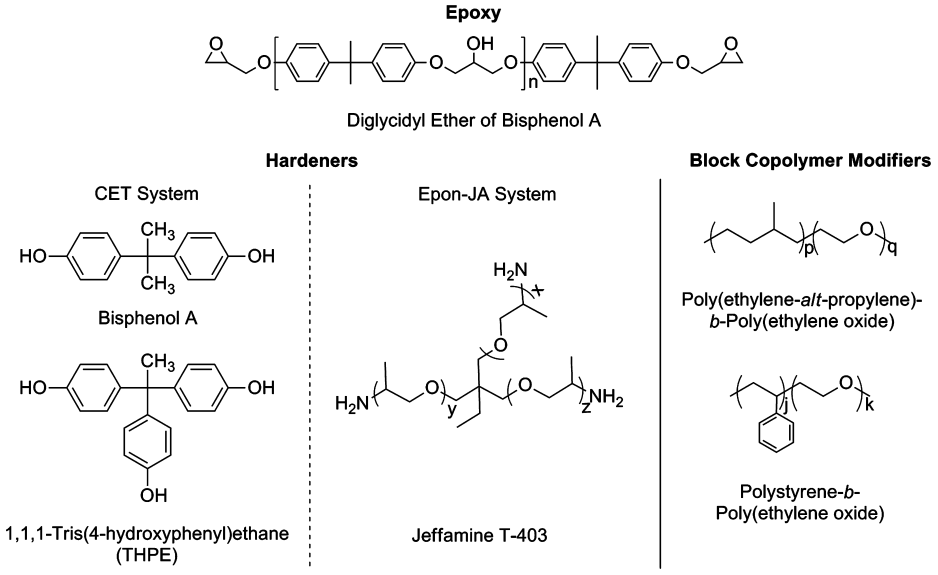


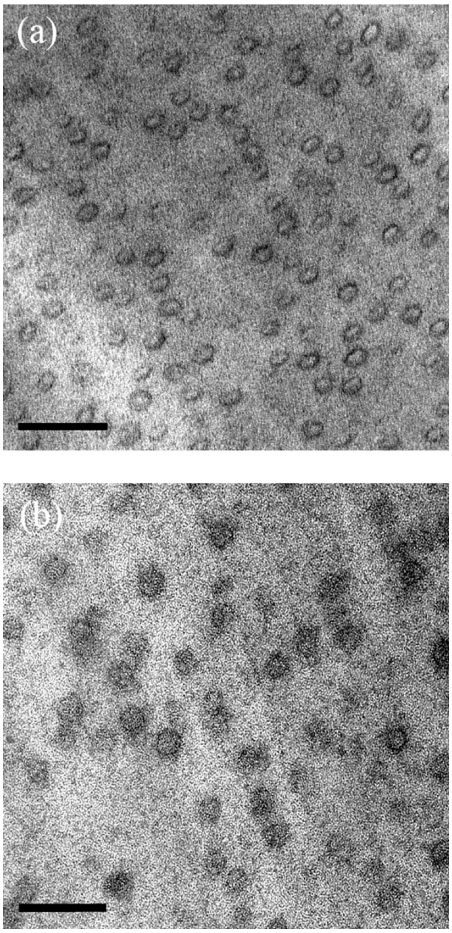


**Figure 1.** Representative TEM images of (a) CET and (b) Epon-JA modified with 5 and 4 wt % block copolymer, respectively. Spherical micelle forming block copolymers with rigid (PS) core were added to both epoxy systems. $RuO_4$, used as contrast agent, preferentially stains the epoxy/micelle interface. Scale bars represent 100 nm.

produces a highly cross-linked network (Chart 1), leading to lower overall values of $G_{1c}$. Here again both types of micelles produce a toughening effect, with the PS-PEO providing roughly half the critical strain energy release rate above a concentration of 1 wt % block copolymer. Interestingly, at low block copolymer content both types of micelles toughen to the same extent. While the toughening effect for the glassy core micelles is independent of concentration, there appears to be a critical block copolymer concentration at which the rubbery core micelles outperform their rigid core counterpart. A detailed discussion on the origins of the toughening trends and their difference in magnitude will be the topic of a separate publication.

With the exception of one CET formulation ($M_c \cong 1850$ g/mol) the glassy spherical micelles afford roughly half the $G_{1c}$ obtained with the rubbery inclusions, above a critical $M_c$ and concentration. Clearly, core cavitation alone cannot explain these results, because glassy PS will not void like rubbery PEP. These results indicate a critical structural parameter outside the micelle core common to both additives. We believe the zone around the core, formed by the PEO corona and associated epoxy, is implicated by these experiments.

We propose that the epoxy/PEO interface, or mixing region, represents the common denominator in rationalizing these results. The effect of the micelle on the properties of the network is depicted in Figure 3. Away from the micelle the epoxy network is completely and uniformly cross-linked. However, the structure and properties of the network in the vicinity of the core are disrupted due to interactions between the epoxy and the PEO corona blocks. We speculate that network disruption results from mixing of PEO with the reacted epoxy in the vicinity of the core.

Prior to curing, the block copolymer micelles are stabilized in the monomer solution by favorable interactions between the PEO corona chains, leading to a random distribution of particles. While we do not know the exact structure of the material in the zone surrounding the micelle core in the cross-linked product, two limiting scenarios can be advanced. In one limit, cross-linking might completely expel the PEO blocks leading to a core−shell structure with nearly pure PEO surrounding the PS or PEP cores. We expect this process would result in some degree of PEO crystallinity. In the opposite extreme, the PEO chains remain mixed with the epoxy matrix, leading to plasticization and/or network damage. Figure 3 illustrates the latter scenario.


dx.doi.org/10.1021/mz200219y | ACS Macro Lett. 2012, 1, 338−342

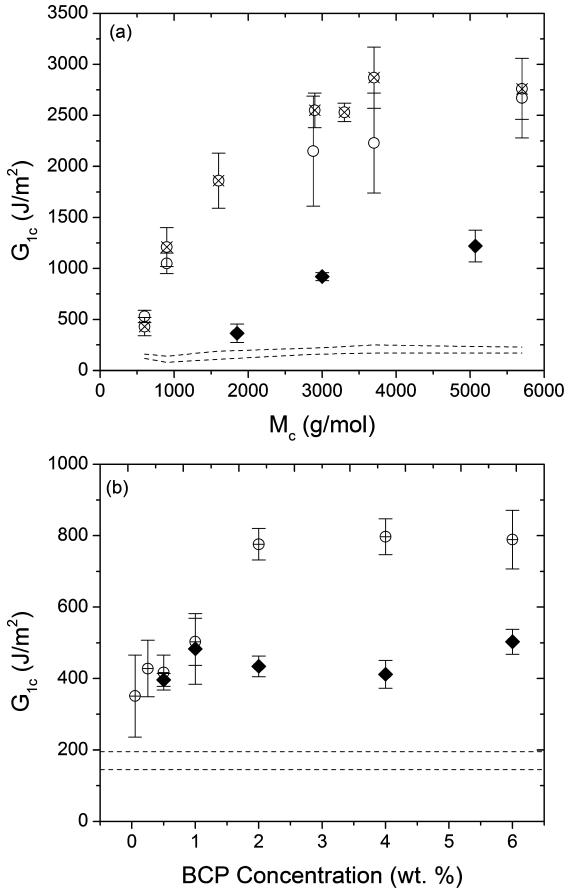


**Figure 2.** Critical strain energy release rate ($G_{1c}$) for (a) CET and (b) Epon-JA epoxy systems. For the CET epoxy system a constant 5 wt % block copolymer loading was used and the molecular weight between cross-links ($M_c$) was varied. For the Epon-JA epoxy system the block copolymer (BCP) concentration effect at a single cross-link density was evaluated. Circles identify rubbery core modifiers: ○ PEP-PEO-1; ⊗ PEP-PEO-2; ⊕ PEP-PEO-3. Filled diamonds identify glassy core modifier: ◆ PS-PEO. Data points indicate the average value of at least five specimens and the error bars represent their standard deviation. Limits of the neat epoxy $G_{1c}$ are represented by the dotted lines. Neat and rubber core data for the CET system are reproduced from Thompson et al.[21]

Models describing structures formed in epoxies with high concentrations of PEO-containing block copolymers,[7,25] later verified experimentally,[26] suggested partial expulsion of the PEO block from the growing network. Formation of discrete domains of PEO with some degree of crystallization should be evidenced by a melting endotherm in a calorimetry experiment. Figure 4a displays DSC traces obtained from Epon-JA modified with PEO homopolymer (Polysciences), PEP-PEO-3, and PS-PEO. The homopolymer is characterized by similar molecular weight as the PEO in the block copolymers and all three specimens contain approximately the same overall amount of PEO. Roughly 5 wt % of the PEO homopolymer is present in a crystalline form (based on an analysis of the small endotherm at 60 °C), while no melting peak is observed in the epoxies modified with block copolymer. The lack of crystallinity in epoxies modified with low concentrations of block copolymer argues against the formation of a discrete layer of PEO close to the core. The DSC traces of the undiluted modifiers, normalized by the mass of PEO, are provided in Figure 4b for reference.

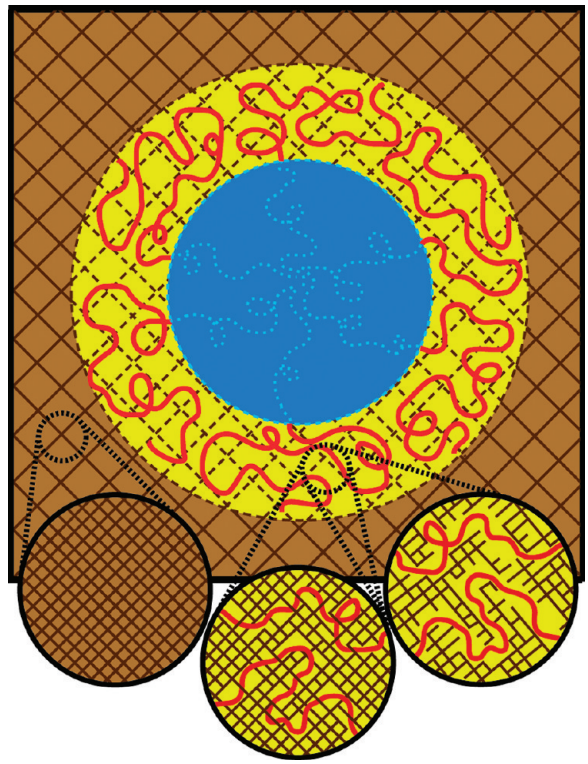

**Figure 3.** Schematic representation of local network disruption and change in properties caused by the presence of the block copolymer micelle in modified epoxies. Different layers of material are depicted: micelle core (blue region), PEO/epoxy interface or mixing region (yellow region with dashed crisscross pattern), and bulk epoxy (brown region with solid crisscross pattern). Away from the micelle (left) the network is fully cross-linked and regular. In the volume spanned by the corona chains two possible scenarios for network disruption are presented: plasticized network (center) and damaged network (right).

We believe that network disruption caused by the corona chains plays a pivotal role in toughening the thermoset epoxies. While matrix shear yielding continues to be the major energy absorbing process during fracture, the proposed network disruption has an analogous role to that previously hypothesized for rubber core cavitation, that is, triggering plastic deformation of the matrix. Consequently, the enhancement in toughness largely depends on the ability of the matrix to shear yield. The relationship between network ductility, cross-link density, and toughenability is well established;[27] the larger the cross-link density of the network the harder it is to enhance fracture resistance. The trends observed in Figure 2a, where smaller $M_c$ is related to a larger cross-link density, are consistent with this notion. Figure 2 also shows that the rubber core clearly outperforms the glassy core, suggesting that the presence of a compliant core enhances the effect of the beneficial disruption caused to the network in the corona region. In other words, a rubbery core amplifies the effect of the triggering mechanism associated with the plasticized and/or damaged zone surrounding both types of micelle.

The results presented here show that rubber core cavitation is not necessary for toughness enhancement in block copolymer modified epoxies; this does not mean that cavitation can be ruled out entirely. An interesting scenario to consider is that of extensive plasticization of the epoxy by the PEO corona in the mixing region. The presence of rubbery PEO chains, as suggested in Figure 4, could produce local regions with subambient


dx.doi.org/10.1021/mz200219y | ACS Macro Lett. 2012, 1, 338−342

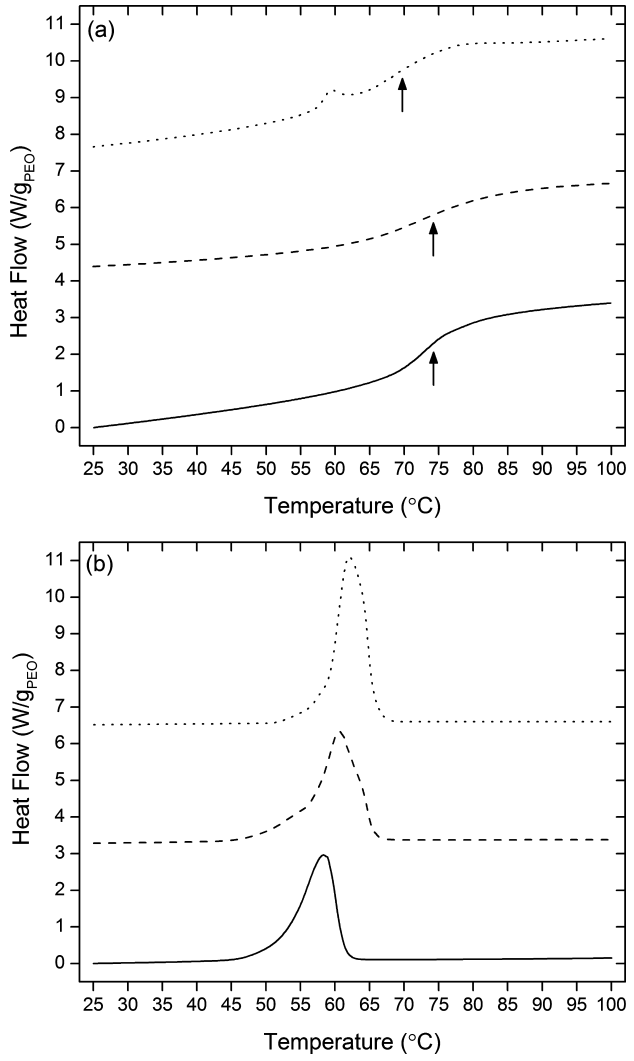


**Figure 4.** DSC traces (exo down) of (a) Epon-JA modified epoxies and (b) bulk modifiers. Epoxies were modified with 3.3, 6, and 6 wt % of PEO homopolymer, PEP-PEO-3, and PS-PEO, respectively. The heat flow was normalized with respect to the mass of PEO in each sample. Solid, dashed, and dotted lines represent PS-PEO, PEP-PEO-3, and PEO homopolymer, respectively. Arrows denote the glass transition temperature of modified epoxies. Curves were shifted vertically for clarity.

glass transition temperature surrounding the micelle cores. In the case of PS-PEO, this rubbery shell adjacent to the glassy core could be prone to cavitation under the high triaxial stress state ahead of the crack tip. Contrary to other epoxy toughening agents, including the PEP-PEO in this work and other types of rubber particles, our PS-PEO modifier was not designed to contain a cavitation prone (rubbery) segment. The possibility of plasticized shell cavitation is a direct consequence of the interaction between the PEO and the epoxy network and supports our argument about the importance of the PEO/epoxy interface unique to this toughening strategy.

Preferential staining of the mixed epoxy/PEO region, evident in Figure 1, supports our conjecture regarding some form of network disruption. $RuO_4$ can react with the aromatic groups in the epoxy network and PS and with the ether groups in PEO.[28] Plasticization or damage caused by the PEO corona likely enhances diffusion and localization of the stain in this portion of the material.

Finally, this new interpretation of block copolymer toughening of epoxies may help explain previous reports of $G_{1c}$ values for worm-like micelles, which are often significantly greater than those obtained with spherical micelles.[15,19,20,29] High aspect ratio cylindrical micelles will engage and modify significantly larger volumes of the cross-linked network, which may facilitate the hypothesized triggering process. Similar reasoning might also account for the recently reported toughness enhancement of epoxies modified with surface-functionalized graphene flakes.[30,31] In this case, even very low concentrations of well-dispersed graphene flakes would create extensive zones of damaged network as the planar geometry of the sheets extends in two dimensions. Additional work is underway to further verify these concepts.

## EXPERIMENTAL METHODS

The polymerization protocols followed in synthesizing PEP-PEO and PS-PEO block copolymers can be found elsewhere.[32,33] Table 1 shows a summary of the molecular characteristics of the block copolymers employed in this study.

**Table 1. Molecular Characterization of Block Copolymers**

| diblock[a,b] | $M_n$ (kg/mol) | $f_{PEO}$[c] | $M_w/M_n$ |
|---|---|---|---|
| PEP-PEO-1[d] | 63.9 | 0.37 | 1.07 |
| PEP-PEO-2[e] | 7.8 | 0.29 | 1.08 |
| PEP-PEO-3 | 27.0 | 0.57 | 1.10 |
| PS-PEO | 56.5 | 0.44 | 1.10 |

[a]PEP = poly(ethylene-*alt*-propylene); PEO = poly(ethylene oxide); PS = polystyrene. [b]PEO is the "epoxy-miscible" block. [c]Volume fraction of PEO calculated using densities at 140 °C.[34] [d]Identified as OP28−36 in Thompson et al.[21] [e]Identified as OP3−5 in Thompson et al.[21]

The first epoxy system (CET) consists of DER 332 (diglycidyl ether of bisphenol A type epoxy monomer with $n$ = 0 (100%), Dow Chemical), bisphenol A (difunctional chain extender, Dow Chemical), and 1,1,1-tris(4-hydroxyphenyl)ethane (trifunctional cross-linker, Aldrich). A complete description and formulation of the CET epoxies has been previously reported.[21,35] CET epoxies were prepared as previously described,[21] except for the PS-PEO modified materials. In this case, the block copolymer was dissolved in acetone at 40 °C, and the solution with all components was heated to 90 °C prior to connection to a vacuum line for solvent removal.

The second epoxy system (Epon-JA) also contains a diglycidyl ether of bisphenol A type epoxy monomer (Epon 828, Polysciences), but with higher oligomer content ($n$ = 0 (88%); $n$ = 1 (10%); $n$ = 2 (2%)). Jeffamine T-403 (aliphatic hexamine with $x + y + z \sim 5.3$, Huntsman) was used as the curing agent. Epon-JA epoxies were prepared by melt blending according to the following procedure. First, the block copolymer was dissolved in the epoxy monomer at elevated temperatures (75 and 110 °C for PEP-PEO and PS-PEO, respectively). Upon full dissolution, the mixture was cooled down to 60 °C and 46 phr (parts per hundred resin) of the curing agent were added. The solution was stirred for 30 min at 60 °C, then degassed in a vacuum oven for 5−10 min and poured into a preheated mold (60 °C). Curing was effected by heating to 60 °C for 40 min followed by 1 h at 80 °C, and finally 2 h at 120 °C after which the oven was turned off and the specimen was allowed to slowly cool to room temperature.

Transmission electron microscopy was used to verify the morphology of the block copolymers in epoxy. Thin sections (ca. 60−80 nm) of cured material were microtomed at room temperature using a Reichert Ultramicrotome S equipped with a diamond knife. Sections were floated on water, transferred to copper grids and stained with the vapor from a 5 wt % $RuO_4$ aqueous solution.[36] Imaging was performed with either a JEOL 1210 or FEI Tecnai G2 Spirit BioTwin electron microscope both at an accelerating voltage of 120 kV.

A linear elastic fracture mechanics approach was used to quantify the toughness of the materials addressed by this study. ASTM standard


dx.doi.org/10.1021/mz200219y | *ACS Macro Lett.* 2012, 1, 338−342

D 5045 was followed to determine sample dimensions and testing procedures. Compact tension specimens were machined from fully cured epoxy plaques. An Instron Testing System (model 1011) operated with a crosshead speed of 10 mm/min was used to apply the uniaxial load. The critical stress intensity factor was calculated from the load at break and sample geometry according to the following equation

$$K_{1c} = \frac{P_{max}}{BW^{1/2}} f\left(\frac{a}{W}\right) \quad (1)$$

where $P_{max}$ is the maximum load in the load−displacement curve, $B$ and $W$ are the thickness and width of the specimen, respectively, $a$ is the initial crack length, and $f(a/W)$ is a geometrical factor found in the ASTM standard. The critical strain energy release rate was evaluated from

$$G_{1c} = (1 - \nu^2)\frac{K_{1c}^2}{E} \quad (2)$$

where $\nu$ (taken as 0.34[37]) and $E$ are the Poisson's ratio and elastic modulus of the material, respectively. The room temperature dynamic elastic modulus ($E'$) was determined using a DMTA IV (Rheometrics) operated with a three-point bending geometry. Samples were subjected to a sinusoidal deformation with strain amplitude of 0.01% at a frequency of 10 rad/s. $G_{1c}$ values are based on the average and standard deviation of at least five specimens.

## AUTHOR INFORMATION


### Corresponding Author

*E-mail: bates001@umn.edu.

### Present Address

[†]DuPont Engineering Research and Technology, DuPont Experimental Station, Wilmington, DE.


### Notes

The authors declare no competing financial interest.

## ACKNOWLEDGMENTS

This work was supported primarily by the MRSEC Program of the National Science Foundation under Award Number DMR-0819885. Part of this work was carried out in the College of Science and Engineering Characterization Facility, University of Minnesota, which has received capital equipment funding from the NSF through the MRSEC, ERC, and MRI programs.

## REFERENCES


(1) Hillmyer, M. A.; Lipic, P. M.; Hajduk, D. A.; Almdal, K.; Bates, F. S. *J. Am. Chem. Soc.* **1997**, *119*, 2749−2750.

(2) Dean, J. M.; Lipic, P. M.; Grubbs, R. B.; Cook, R. F.; Bates, F. S. *J. Polym. Sci., Part B: Polym. Phys.* **2001**, *39*, 2996−3010.

(3) Kosonen, H.; Ruokolainen, J.; Nyholm, P.; Ikkala, O. *Macromolecules* **2001**, *34*, 3046−3049.

(4) Guo, Q.; Thomann, R.; Gronski, W.; Staneva, R.; Ivanova, R.; Stuhn, B. *Macromolecules* **2003**, *36*, 3635−3645.

(5) Rebizant, V.; Abetz, V.; Tournilhac, F.; Court, F.; Leibler, L. *Macromolecules* **2003**, *36*, 9889−9896.

(6) Ritzenthaler, S.; Court, F.; David, L.; Girard-Reydet, E.; Leibler, L.; Pascault, J. P. *Macromolecules* **2002**, *35*, 6245−6254.

(7) Lipic, P. M.; Bates, F. S.; Hillmyer, M. A. *J. Am. Chem. Soc.* **1998**, *120*, 8963−8970.

(8) Ritzenthaler, S.; Court, F.; Girard-Reydet, E.; Leibler, L.; Pascault, J. P. *Macromolecules* **2003**, *36*, 118−126.

(9) Guo, Q.; Chen, F.; Wang, K.; Chen, L. *J. Polym. Sci., Part B: Polym. Phys.* **2006**, *44*, 3042−3052.

(10) Fine, T.; Lortie, F.; David, L.; Pascault, J.-P. *Polymer* **2005**, *46*, 6605−6613.

(11) Hermel-Davidock, T. J.; Tang, H. S.; Murray, D. J.; Hahn, S. F. *J. Polym. Sci., Part B: Polym. Phys.* **2007**, *45*, 3338−3348.

(12) Maiez-Tribut, S.; Pascault, J. P.; Soulé, E. R.; Borrajo, J.; Williams, R. J. J. *Macromolecules* **2007**, *40*, 1268−1273.

(13) Hydro, R. M.; Pearson, R. A. *J. Polym. Sci., Part B: Polym. Phys.* **2007**, *45*, 1470−1481.

(14) Dean, J. M.; Grubbs, R. B.; Saad, W.; Cook, R. F.; Bates, F. S. *J. Polym. Sci., Part B: Polym. Phys.* **2003**, *41*, 2444−2456.

(15) Dean, J. M.; Verghese, N. E.; Pham, H. Q.; Bates, F. S. *Macromolecules* **2003**, *36*, 9267−9270.

(16) Guo, Q.; Dean, J. M.; Grubbs, R. B.; Bates, F. S. *J. Polym. Sci., Part B: Polym. Phys.* **2003**, *41*, 1994−2003.

(17) Liu, J. D.; Sue, H.-J.; Thompson, Z. J.; Bates, F. S.; Dettloff, M.; Jacob, G.; Verghese, N.; Pham, H. *Macromolecules* **2008**, *41*, 7616−7624.

(18) Liu, J. D.; Sue, H.-J.; Thompson, Z. J.; Bates, F. S.; Dettloff, M.; Jacob, G.; Verghese, N.; Pham, H. *Polymer* **2009**, *50*, 4683−4689.

(19) Wu, J.; Thio, Y. S.; Bates, F. S. *J. Polym. Sci., Part B: Polym. Phys.* **2005**, *43*, 1950−1965.

(20) Thio, Y. S.; Wu, J.; Bates, F. S. *Macromolecules* **2006**, *39*, 7187−7189.

(21) Thompson, Z. J.; Hillmyer, M. A.; Liu, J. D.; Sue, H.-J.; Dettloff, M.; Bates, F. S. *Macromolecules* **2009**, *42*, 2333−2335.

(22) Rebizant, V.; Venet, A.-S.; Tournilhac, F.; Girard-Reydet, E.; Navarro, C.; Pascault, J.-P.; Leibler, L. *Macromolecules* **2004**, *37*, 8017−8027.

(23) Yang, X.; Yi, F.; Xin, Z.; Zheng, S. *Polymer* **2009**, *50*, 4089−4100.

(24) The images presented in Figure 1 correspond to the case of epoxies modified with polystyrene core micelles. Micrographs of the epoxies modified with poly(ethylene-*alt*-propylene) core micelles closely resembled those of previous work, and hence not included here. The reader is directed to ref 21 for examples of such images.

(25) Mijovic, J.; Shen, M.; Sy, J. W.; Mondragon, I. *Macromolecules* **2000**, *33*, 5235−5244.

(26) Sun, P.; Dang, Q.; Li, B.; Chen, T.; Wang, Y.; Lin, H.; Jin, Q.; Ding, D.; Shi, A.-C. *Macromolecules* **2005**, *38*, 5654−5667.

(27) The influence of matrix ductility has been extensively considered when reviewing epoxy toughening strategies. See, for example, Bagheri, R.; Marouf, B. T.; Pearson, R. A. *Polym. Rev.* **2009**, *49*, 201−225.

(28) Trent, J. S.; Scheinbeim, J. I.; Couchman, P. R. *Macromolecules* **1983**, *16*, 589−598.

(29) Liu, J. D.; Thompson, Z. J.; Sue, H.-J.; Bates, F. S.; Hillmyer, M. A.; Dettloff, M.; Jacob, G.; Verghese, N.; Pham, H. *Macromolecules* **2010**, *43*, 7238−7243.

(30) Rafiee, M. A.; Rafiee, J.; Wang, Z.; Song, H.; Yu, Z.-Z.; Koratkar, N. *ACS Nano* **2009**, *3*, 3884−3890.

(31) Rafiee, M. A.; Rafiee, J.; Srivastava, I.; Wang, Z.; Song, H.; Yu, Z.; Koratkar, N. *Small* **2010**, *6*, 179−183.

(32) Hillmyer, M. A.; Bates, F. S. *Macromolecules* **1996**, *29*, 6994−7002.

(33) Bailey, T. S.; Pham, H. D.; Bates, F. S. *Macromolecules* **2001**, *34*, 6994−7008.

(34) Fetters, L. J.; Lohse, D. J.; Richter, D.; Witten, T. A.; Zirkel, A. *Macromolecules* **1994**, *27*, 4639−4647.

(35) Sherman, C. L.; Zeigler, R. C.; Verghese, N. E.; Marks, M. J. *Polymer* **2008**, *49*, 1164−1172.

(36) Khandpur, A. K.; Macosko, C. W.; Bates, F. S. *J. Polym. Sci., Part B: Polym. Phys.* **1995**, *33*, 247−252.

(37) Grillet, A. C.; Galy, J.; Gérard, J.-F.; Pascault, J.-P. *Polymer* **1991**, *32*, 1885−1891.